

Evaluation of respiratory disease hospitalisation forecasts using synthetic outbreak data

Grégoire Béchade^{1,*}, Torbjörn Lundh², and Philip Gerlee³

¹Ecolé Polytechnique, gregoire.bechade@polytechnique.edu

²Department of Mathematical Sciences, Chalmers University of Technology & University of
Gothenburg, Sweden, torbjorn.lundh@chalmers.se

³Department of Mathematical Sciences, Chalmers University of Technology & University of
Gothenburg, Sweden gerlee@chalmers.se

*Corresponding author: Grégoire Béchade

Abstract

Forecasts of hospitalisations of infectious diseases play an important role for allocating healthcare resources during epidemics and pandemics. Large-scale analysis of model forecasts during the COVID-19 pandemic has shown that the model rank distribution with respect to accuracy is heterogeneous and that ensemble forecasts have the highest average accuracy. Building on that work we generated a maximally diverse synthetic dataset of 324 different hospitalisation time-series that correspond to different disease characteristics and public health responses. We evaluated forecasts from 14 component models and 6 different ensembles. Our results show that component model accuracy was heterogeneous and varied depending on the current rate of disease transmission. Going from 7 day to 14 day forecasts mechanistic models improved in relative accuracy compared to statistical models. A novel adaptive ensemble method outperforms all other ensembles, but is closely followed by a median ensemble. We also investigated the relationship between ensemble error and variability of component forecasts and show that the coefficient of variation is predictive of future error. Lastly, we validated the results on data from the COVID-19 pandemic in Sweden. Our findings have the potential to improve epidemic forecasting, in particular the ability to assign confidence to ensemble forecasts at the time of prediction based on component forecast variability.

Keywords: infectious disease modelling, forecast, evaluation, ensemble model.

1. Introduction

Prediction of future outcomes such as incidence, hospital admissions and mortality, plays an important role in infectious disease epidemiology (Lutz et al., 2019), both in terms of

short-term prediction or forecasts and longer-term scenario projections. The time-scales 33
relevant for forecasting and projections depends on the characteristics of the disease, but it 34
is generally acknowledged that the accuracy of forecasts degrade rapidly beyond a month 35
(Cramer et al., 2022). This depends both on the inherently non-linear nature of disease 36
transmission and on potential rapid changes in processes relevant for transmission, e.g. 37
altered contact rates due to enforced or voluntary social distancing (Fox et al., 2022; 38
Gerlee et al., 2021). 39

Forecasts of key epidemiological variables have played an important role in a number 40
disease outbreaks including Zika virus (Kobres et al., 2019), Ebola (Munday et al., 2024), 41
Seasonal Influenza (Reich et al., 2019) and COVID-19 (Cramer et al., 2022). The utility 42
of infectious disease forecasts ranges from informing decision-makers about the future 43
developments of the epidemic, to the distribution of medical supplies and supporting the 44
allocation of health-care resources. 45

Forecasting models require historical data in order to produce useful forecasts. While 46
mortality data typically remains stable during an epidemic it is often subject to report- 47
ing delays and in addition there is typically a delay of several weeks from infection to 48
death, which can hamper forecasting efforts. Incidence data on the other hand does not 49
suffer from this drawback, but is instead affected by testing strategies, which can vary 50
significantly during the course of an epidemic. It has been argued that hospital admis- 51
sion present a useful middle-ground since admission criteria are more stable and forecasts 52
of hospitalisations are valuable for regional decision-makers and allocation of healthcare 53
resources, such as ICU-beds (Fox et al., 2022). 54

For these purposes a whole range of different forecasting models have been utilised, 55
ranging from statistical models, mechanistic/compartamental models in terms of ordinary 56
differential equations to agent-based models (Nixon et al., 2022). This diversity of ap- 57
proaches became obvious during the COVID-19 pandemic and was particularly highlighted 58
through the efforts of a number of forecast hubs where research groups and individuals 59
alike could submit forecasts on a regular basis as well as documentation and code of their 60
model (Reich et al., 2022). Most prominent of these initiatives was the US COVID-19 61
Forecast Hub (Cramer et al., 2021) which operated from spring 2020 until the autumn 62
2023 and focused on forecasts of mortality and hospitalisations at both the national and 63
state level in the US. 64

An evaluation carried out on forecasts of mortality submitted to the US Forecast Hub 65
showed large heterogeneity in performance among the 27 models that were considered 66
(Cramer et al., 2022). Approximately two-thirds of the models performed better than a 67
naïve baseline model and no single model outperformed the others. Instead it was observed 68
that an ensemble of model forecasts performed best on average. The hub ensemble was 69
to begin with formed by taking an unweighted average of point predictions and quantile 70
levels of the submitted forecasts, but was later changed into an ensemble formed from the 71
median of the component forecasts. 72

Other methods for forming an ensemble have also been considered, e.g. optimising the weights of the models with respect to the performance of component models on historical data (Ray et al., 2021). While this improves performance relative to an unweighted mean the performance is similar to a median ensemble (Brooks et al., 2020), which is both conceptually easier to communicate and computationally easier to calculate. However, there is currently no theoretical basis for choosing component models in an optimal way, nor a theoretical understanding of why certain ensembles perform better than others.

Thus, there is a need to better understand the performance of both individual models and ensemble forecasts. One approach to this problem is to evaluate models and ensembles in a large-scale epidemic dataset, and while the evaluation of the US Forecast Hub contains large number of individual forecasts they are not independent since they concern geographical locations with similar transmission dynamics. Our goal here is to develop a novel method for evaluating epidemiological forecasting models, that utilises synthetically generated diverse data that reflects both different disease characteristics and responses to the epidemic in terms of time-dependent mobility.

In order to further our understanding of epidemic forecasting we present a large-scale and maximally diverse dataset of hospital admissions against which forecast models can be tested. We have characterised the performance of 14 different component models ranging from statistical to mechanistic models and covering both univariate and multivariate models. We also evaluated six different ensemble models and present a novel adaptive ensemble which utilises information about the current transmission dynamics. Lastly, our large-scale approach offers new insight into the relationship between the error of ensemble forecasts and the variance of component forecasts, information that can be used to judge the reliability of ensembles.

2. Results

2.1 Overview of the approach

In order to generate synthetic data on hospitalisations from an epidemic we made use of CovaSim (Kerr et al., 2021) an agent-based model of COVID-19 transmission, where disease and transmission parameters can be tuned to represent a wide-range of respiratory tract infections with e.g. different severity profiles, serial interval distributions and fraction of asymptomatics. The transmission dynamics can also be modulated by specifying time-dependent mobility rates.

In the simulation we consider all cases that are severe and critical to require hospital admission and extract the number of hospitalised patients each day of the simulation. In addition to hospitalisations we also record the incidence, the effective reproduction number and mobility each day.

To generate a maximally diverse set of epidemics we constructed a metric that quantifies the difference between hospitalisation curves and made use of a Markov Chain

Monte Carlo-method for identifying the subset of parameters, which when varied give 111
rise to diverse epidemics (see figure 1A and Methods). We identified four parameters 112
(symptomatic-to-severe rate, asymptomatic-to-recovered rate, probability of being symp- 113
tomatic, probability of becoming severe) that when varied had the largest impact on the 114
epidemic. We ran CovaSim with all possible parameters combinations when each para- 115
meter was either halved, at baseline or doubled. In addition we considered four different 116
time-dependent mobility rates: seasonal, lockdowns, empirical and constant. This yielded 117
324 unique epidemics each 300 days long (see figure 1B). 118

On each epidemic we trained 14 different forecast models and every 20 days we made 119
forecasts of the number of hospitalised cases 7 and 14 days ahead (see figure 1C). We 120
considered statistical models (e.g. exponential regression), autoregressive models (e.g. 121
ARIMA) and mechanistic models (e.g. a SIRH-model which is an extension of the SIR- 122
model with a compartment for hospitalised cases). Some models were univariate and only 123
used the past hospitalisations to forecast the future, whereas others were multivariate and 124
used past mobility and incidence for forecasting (e.g. a multivariate exponential regression 125
and a VAR-model). We refer to the Methods for a detailed description of all models. The 126
performance of the models was evaluated using both root mean squared error (RMSE) and 127
the weighted interval score (WIS) (Bracher et al., 2021) (see Methods). 128

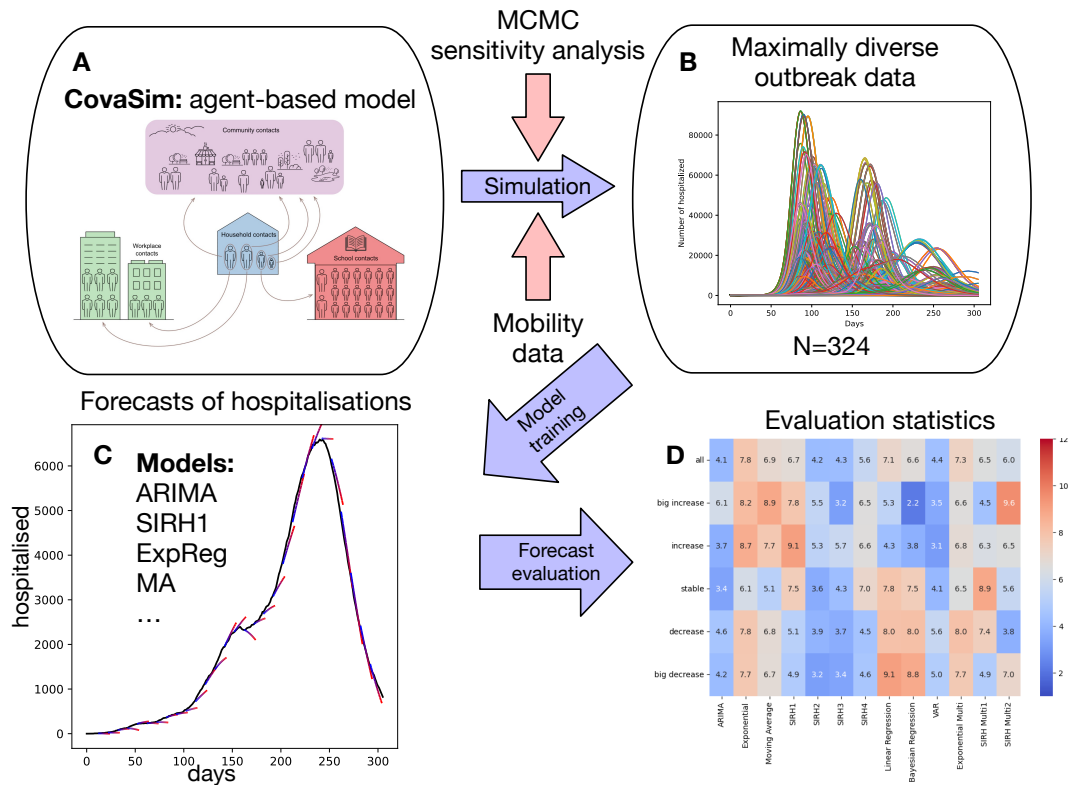


Figure 1: Overview of the methodology. A) We identified parameters in CovaSim, which when varied, gave rise to the most diverse set of outbreak data. B) Using these parameters we generated 324 different daily time-series of the number of hospitalised patients each X days long. C) 13 different forecasting models were trained on each time-series and the accuracy of 7 and 14 days ahead predictions was evaluated using RMSE and WIS. D) Results were aggregated and the models were ranked based on accuracy.

2.2 Performance of individual models

129

Point forecasts of all considered models on an example epidemic are shown in figure 2. 130
 Here it can be seen that some models appear to provide accurate point forecast (e.g. the 131
 ARIMA- and VAR-models), whereas others such as the SIRH-1 and ExpMultiReg fail to 132
 provide good forecasts. 133

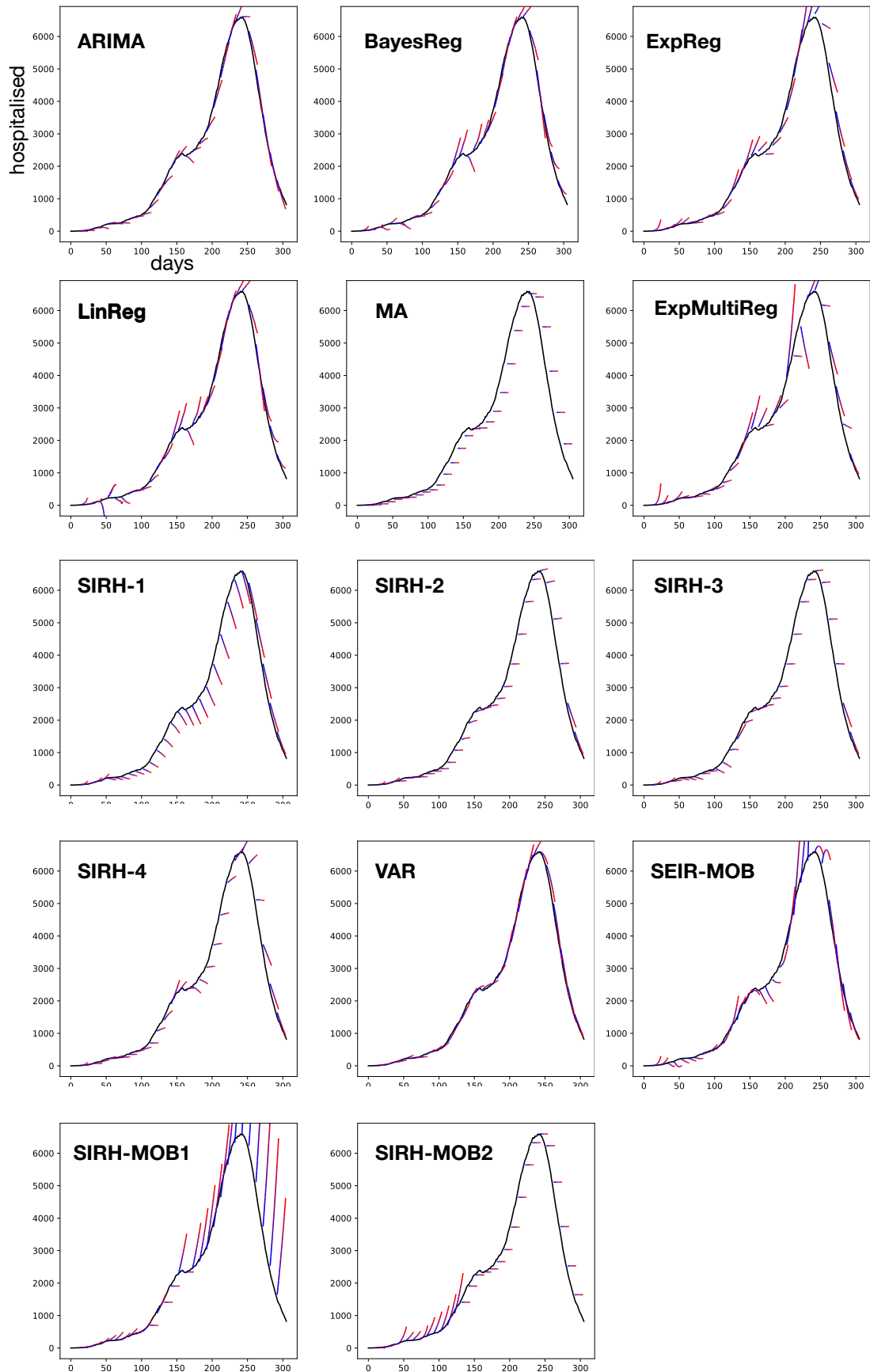


Figure 2: Forecasts of all models on a single example epidemic. Forecast are made every 10 days, starting at day 10, and stretch 14 days ahead. The colouring of the forecast curves indicates the length of the forecast (blue at day 0 and red at day 14).

In order to systematically investigate the accuracy of the models across all 324 epidemics we calculated the RMSE and WIS of each forecast and ranked the models according to their performance. The distribution of ranks based on RMSE and WIS is shown in figure 3, where height of the bars correspond to the fraction of times each model achieved the corresponding rank. The Moving Average (MA) model represents our baseline model and forecasts the average number of hospitalised cases in 7 day period prior to the day of forecast. As expected this model performs poorly with respect to both the WIS and RMSE metrics, although it does perform best in a small fraction of cases. In fact for most models the rank distribution with respect to WIS and RMSE are similar, the exception being the Exponential Regression model. This discrepancy arises because the ExpReg-model provides accurate point predictions, but (at times) excessively wide confidence intervals, which increases the WIS and places the model at the bottom of the ranking. The rank distribution for 7 day forecast is similar (see fig. S1).

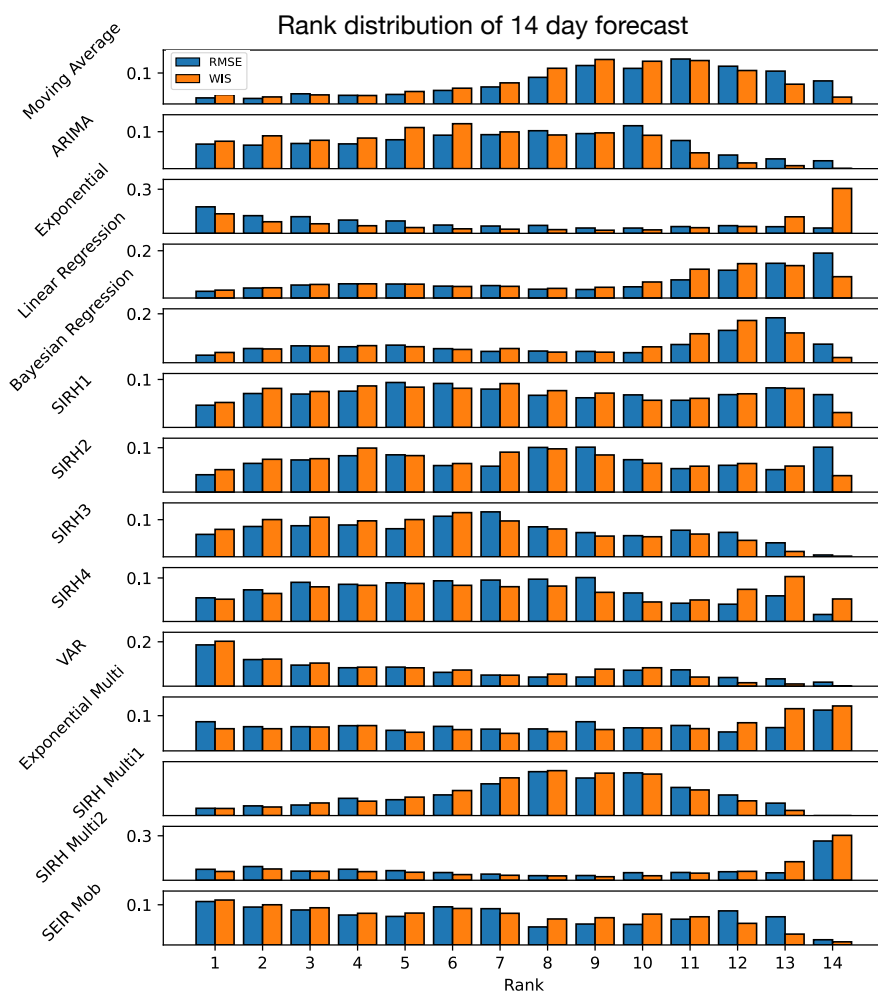


Figure 3: Distribution of rankings of the models for all points for 14-day forecasts with respect to both RMSE and WIS. The average ranks for each model is reported in Table 1

The rank distribution can be summarised by considering the average ranks of the models, which is shown in Table 1. To begin with note that the MA-models has the worst

average rank in all cases except for WIS at 14 days where SIRH-Multi2 and ExpReg perform worse. We can see that the top performing models with respect to RMSE for 7 days is VAR, ExpReg and ARIMA, and for 14 days we have ExpReg, VAR and SEIR-Mob. If we instead consider WIS the top performing models for 7 days are VAR, ARIMA and SIRH3, and for 14 days forecasts: VAR, SIRH3 and ARIMA. It is worth noting that the top models contain both statistical and mechanistic models. If we consider the change in rank going from 7 to 14 days we see that all models that have an autoregressive structure (ARIMA, LinReg, BayesReg and VAR) perform worse for longer forecast horizons. This is true for both WIS and RMSE. On the contrary all mechanistic models perform better at 14 days compared to 7 days (for both RMSE and WIS). The latter also holds true for the Moving Average-model and the two exponential regression models.

Model	RMSE (7 days)	WIS (7 days)	RMSE (14 days)	WIS (14 days)
Moving Average	10.60	9.69	9.50	8.83
ARIMA	6.15	5.40	7.00	6.07
Exponential	5.72	8.70	5.57	8.62
Linear Regression	8.04	7.61	9.41	9.01
Bayesian Regression	7.17	6.82	8.71	8.34
SIRH1	7.94	7.57	7.52	7.16
SIRH2	8.37	7.60	7.73	7.13
SIRH3	6.97	6.10	6.64	5.93
SIRH4	7.28	8.15	6.75	7.44
VAR	5.09	4.64	5.58	5.03
Exponential Multi	7.81	8.62	7.67	8.29
SIRH Multi1	8.65	8.35	8.00	7.74
SIRH Multi2	8.49	9.49	8.34	9.23
SEIR Mob	6.72	6.27	6.57	6.17

Table 1: Average rank of all 14 models for 7- and 14-day forecasts with respect to RMSE and WIS in order of increasing error.

We then went on to stratify the average ranks based on the characteristic of the epidemic in terms of the effective reproductive number R_{eff} at the day the forecast was made. We consider five different classes ranging from minimal transmission ($R_{\text{eff}} < 0.5$), low transmission ($0.5 \leq R_{\text{eff}} < 0.8$) to stable ($0.8 \leq R_{\text{eff}} < 1.2$), high transmission ($1.2 \leq R_{\text{eff}} < 3$) and very high transmission $R_{\text{eff}} \geq 3$. The results can be seen in figure 4 which shows the average rank using WIS at 14 days. It is clear that model performance in general is quite heterogeneous with respect to R_{eff} . For example the VAR-model performs very well at times of high and very high transmission (average rank of 2.6 and 2.8 respectively) but considerably worse at low transmission (average rank 6.3), where it is outperformed by six other models. On the other hand the SEIR-Mob model is the best model during minimal transmission (average rank 3.6), but is outperformed by seven other models during high transmission (results for WIS 7 days and RMSE for 7 and 14 day forecasts are similar, see fig. S2). This suggest that knowledge about the current status of the

epidemic can inform model choice, a fact we will return to when constructing ensemble models.

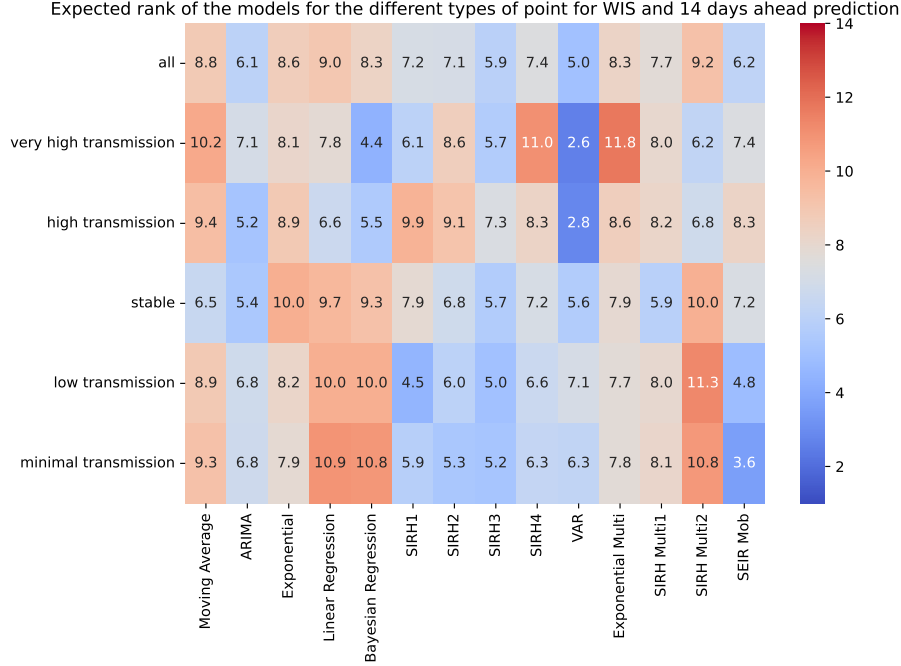


Figure 4: Heatmap of model performance based on WIS for 14-day forecasts. The day of forecast is classified according to the current effective reproduction number according to: minimal transmission ($R_{\text{eff}} < 0.5$), low transmission ($0.5 \leq R_{\text{eff}} < 0.8$), stable ($0.8 \leq R_{\text{eff}} < 1.2$), high transmission ($1.2 \leq R_{\text{eff}} < 3$) and very high transmission $R_{\text{eff}} \geq 3$.

As noted earlier some models make use of multivariate data to make forecasts of future hospitalisations. These additional data streams in terms of incidence and mobility are provided to the models at the same daily resolution as the hospitalisation data. In a sense this makes for an unfair comparison between univariate and multivariate models since incidence and mobility data rarely is available at such high temporal resolution. In order to investigate the impact of the temporal resolution of the additional data streams we reduced the resolution in a range from daily to every 30 days. Historical data was linearly interpolated and care was taken not to use data beyond the date of forecast during interpolation. We then calculated the performance in terms of average WIS across all epidemics. This was carried out for the VAR and SEIR-Mob models, which both performed well compared to the other models, and the result can be seen in figure 5. For the VAR-model, which uses both incidence and mobility, the performance decreases (corresponding to an increase in WIS) approximately linearly from a daily temporal resolution to a resolution of roughly 20 days at which point the performance saturates. For reference the average WIS of the Moving Average model equals 1475, which is above the WIS of the VAR-model for all resolutions. In contrast the SEIR-Mob model, which uses mobility data, performs even better (i.e. lower WIS) when the resolution is increased to 10 days and from then on the WIS remains roughly constant. A possible explanation for this

is that for one of the mobility datasets the mobility changes on a weekly basis and the linear interpolation employed to reduce the resolution in fact improves the utility of the data. In conclusion, these results suggest that in realistic scenarios where incidence and mobility are available on a weekly resolution (or less) the mechanistic SEIR-Mob model is preferable compared to the autoregressive VAR-model.

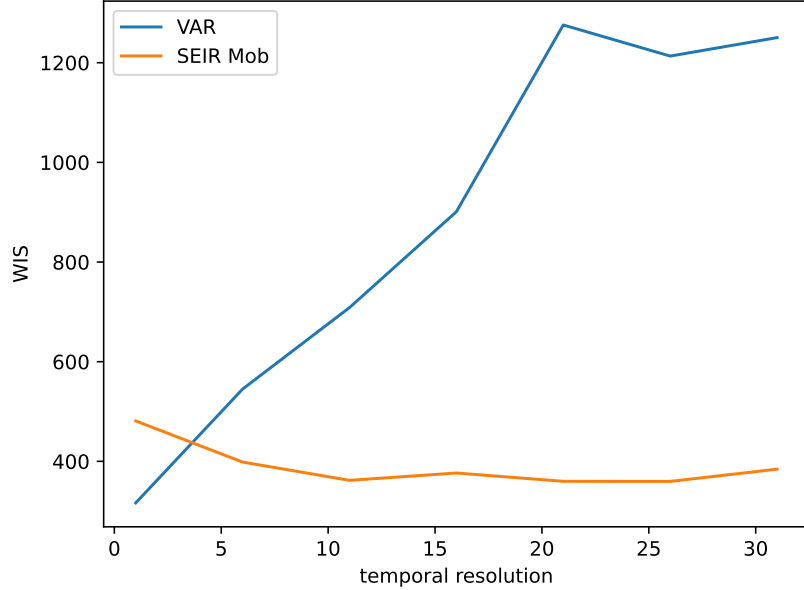


Figure 5: Performance of the VAR- and SEIR Mob-model as the temporal granularity is decreased. At temporal granularity of $T = 1$ the models utilise daily prevalence and mobility data, whereas for higher granularity the data is available every T days. For reference the average WIS of the baseline MA-model equals 1475.

2.3 Ensemble model

It has been established that ensemble forecasts typically outperform component models in terms of performance (Taylor & Taylor, 2023). We investigate this observation in the context of our large-scale synthetic dataset and consider the following types of ensembles:

- Average Ensemble (EnsAvg): this ensemble takes an unweighted mean of all component models to calculate the point prediction and confidence intervals (Cramer et al., 2022).
- Median Ensemble (EnsMedian): this ensemble uses the median of all point predictions and confidence intervals (Ray et al., 2023).
- Regression Ensemble (EnsReg): this ensemble takes a weighted mean of the component point predictions and confidence intervals plus an intercept. The weights and intercept were obtained using linear regression where the component model forecasts are covariates and the actual hospitalisation is the target variable.

- RMSE-optimised Ensemble (EnsRMSE): same as EnsReg with the difference that the weights are constrained to sum to unity and there is no intercept (Brooks et al., 2020).
- WIS-optimised Ensemble (EnsWIS): same as EnsRMSE but here the weights are selected to minimise the WIS of the ensemble forecast. Again the weights sum to unity (Brooks et al., 2020).
- Rank-based Ensemble (EnsRank): this ensemble changes its weights depending on the current effective reproductive number. For each of the five regimes defined in fig. 4 we pick the five models with the smallest average rank. The weights of the models are set to the inverse of the model rank, and lastly the weights are normalised to sum to unity, similar to what is done in (Taylor & Taylor, 2023).

The model weights were obtained by splitting the epidemics into a training and evaluation set and calibrating the weights on the training set. The resulting model weights are shown in fig. 6.

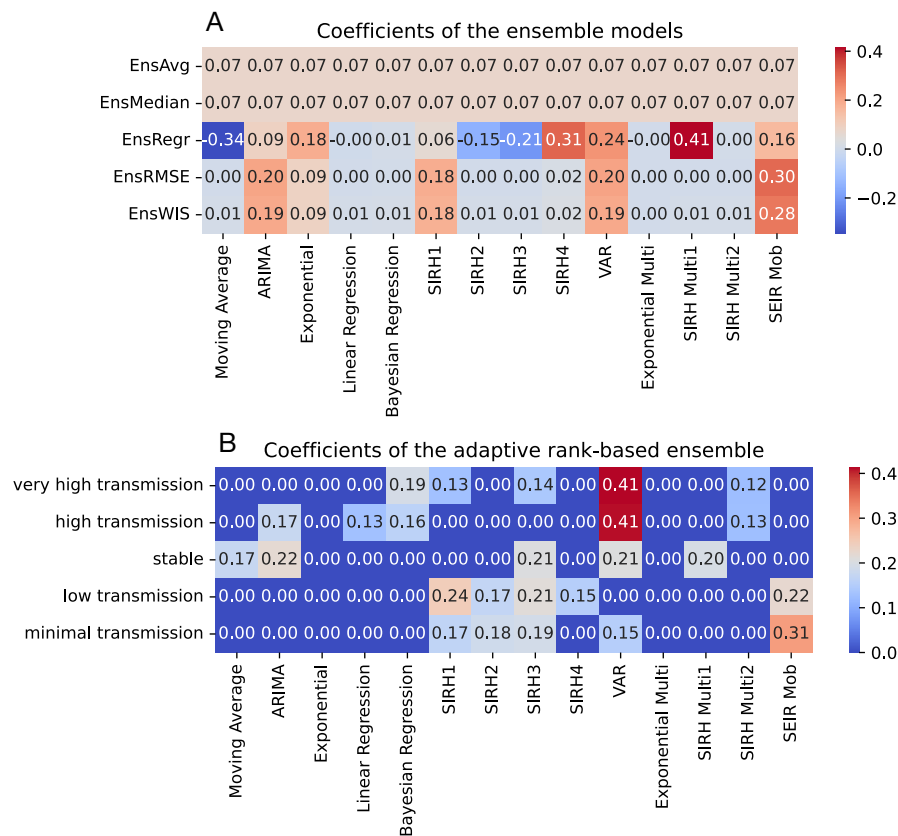


Figure 6: A. The weights of component model predictions in the ensembles. Note that for the Median Ensemble (EnsMedian) the point prediction is given as the median of the model predictions. This also applies to the quantiles of the EnsMedian-prediction. B. The weights in the rank-based adaptive ensemble that are chosen depending on the current effective reproductive number.

We then evaluated the performance of the ensembles on the evaluation set with respect to both WIS and RMSE. The average rank of the ensembles when compared to all models (in total 20 models, 14 component models plus 6 ensembles) is shown in fig. 7. In terms of RMSE-performance the ensembles do not outperform the component models when considering all points, but do so for some types of points, e.g. EnsRank has the lowest average rank for 'low transmission' and EnsMedian has the lowest average rank when transmission is 'stable' (see fig. S3 for a comparison of all models and ensembles). However, for WIS-performance the picture is different. Here three ensembles, EnsMedian, EnsWIS and EnsRank, clearly outperform all component models and other ensembles. EnsRank has the lowest overall rank for all transmission regimes except 'high transmission', where EnsMedian has the lowest average rank.

In situations where component models in an ensemble agree it is reasonable to think that the ensemble should be more accurate compared to a situation where component predictions diverge. To investigate this hypothesis we measured the accuracy of the median ensemble in terms of the mean absolute percentage error (MAPE) and compared it to the coefficient of variation (CV) of the component forecast. CV is calculated as the sample standard deviation divided by the sample mean and is a normalised measure of variation within a sample. Figure 8 shows a scatter plot of the MAPE and CV of each individual forecast for all epidemics together with the mean and standard deviation of binned data. From the plot it is clear that a small CV implies a small MAPE, whereas for large CVs the MAPE can take a range of values. Although the data has a strong heteroscedastic trend we observe an increased mean MAPE as the CV of the ensemble increases. This implies that the CV of the ensemble is predictive of future error of the ensemble forecast.

2.4 Evaluation on real data

To validate our findings concerning the performance different ensembles we trained the models and made forecasts of hospitalised COVID-19 patients during 2020 in Sweden. We calculated the WIS for the top two component models (ARIMA and VAR) and ensembles (EnsMedian and EnsRank). The results are shown in fig. 9 together with the instantaneous reproductive number estimated from incidence data (Cori et al., 2013), which is used by the rank-based ensemble. Also here we see that the ensemble forecasts achieve lower WIS and EnsRank achieves a slightly lower WIS compared to EnsMedian (73.8 vs. 77.4).

3. Discussion

We have investigated the ability of a wide array of forecasting models to predict the number of hospitalised cases of a hypothetical respiratory infectious disease. A diverse set of outbreak data was generated using CovaSim, an established agent-based model of

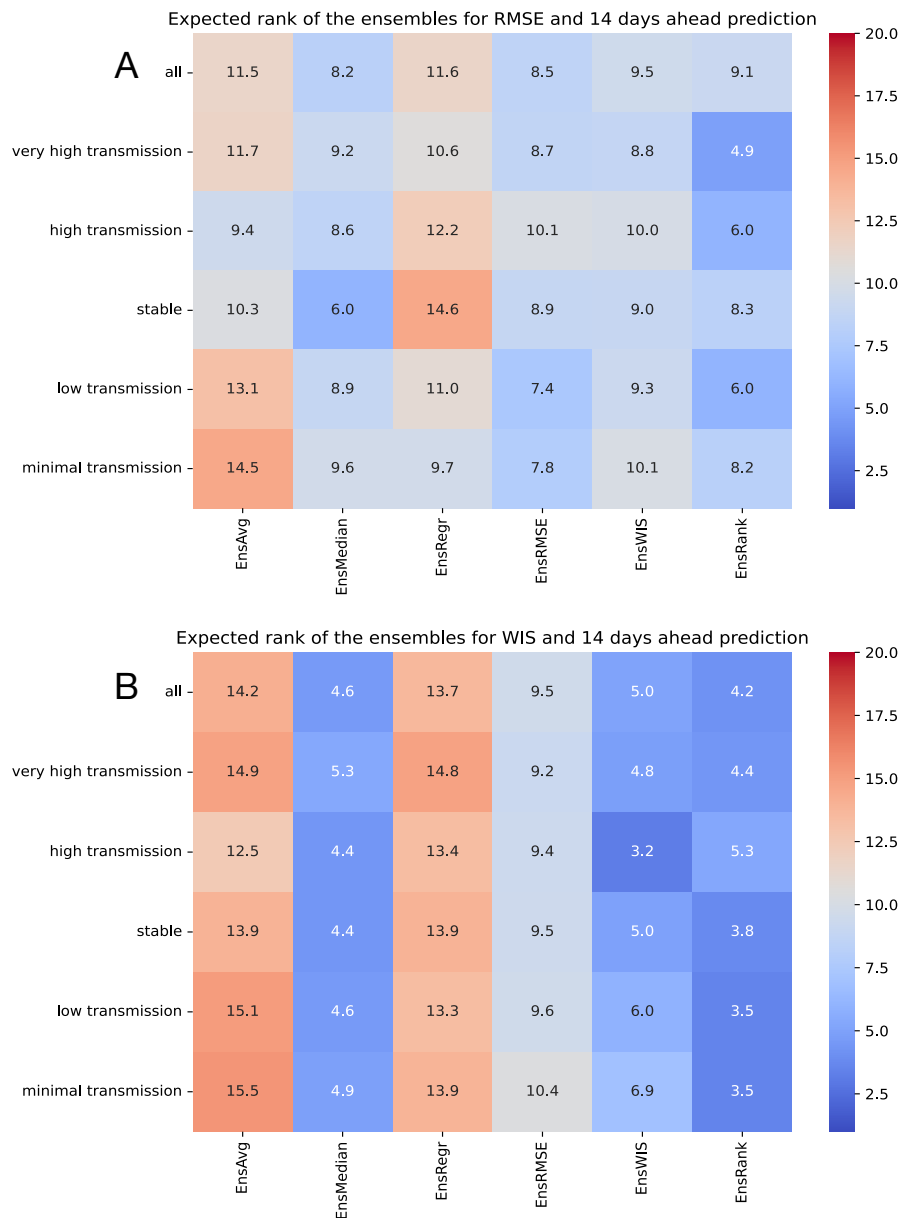


Figure 7: The average ensemble rank as compared to both component models and the six ensembles for A) RMSE and B) WIS.

COVID-19 transmission, whose parameters were adjusted to generate a maximally diverse set of hospitalisation curves (see 1B).

We considered 14 forecasting models that were either autoregressive, statistical or mechanistic and were univariate or multivariate (made use of multiple data types for prediction). The accuracy of the models was evaluated using both RMSE (for point predictions) or WIS (for probabilistic predictions) for 7- and 14-day forecasts. For each forecast we ranked the models according to their RMSE/WIS with the first ranked model having the lowest error. The resulting rank distributions (fig. 3) based on all epidemics and forecasts (in total 4860 points) are highly heterogeneous were no model consistently outperforms the others. Similar findings have been made by forecast hubs during the

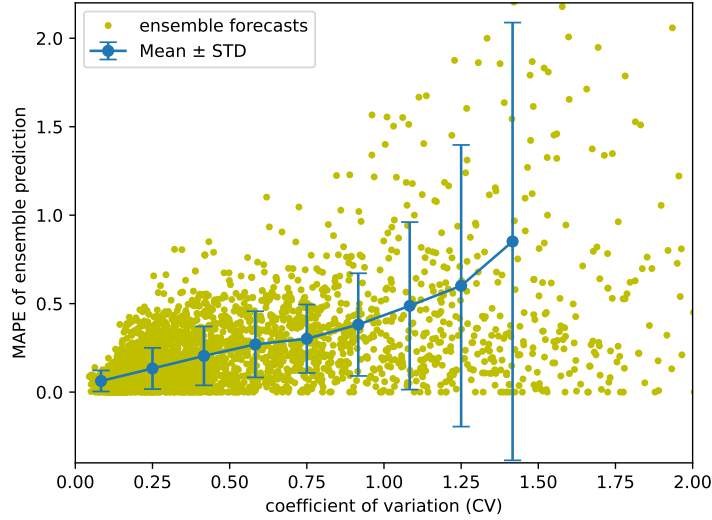


Figure 8: The coefficient of variation (CV) of the individual model predictions for 7-day forecasts and the corresponding error (MAPE) of the Median Ensemble prediction. The solid line shows the mean MAPE in each bin and the error bars correspond to one standard deviation (see fig. S4 for the corresponding plot for 14 day forecasts).

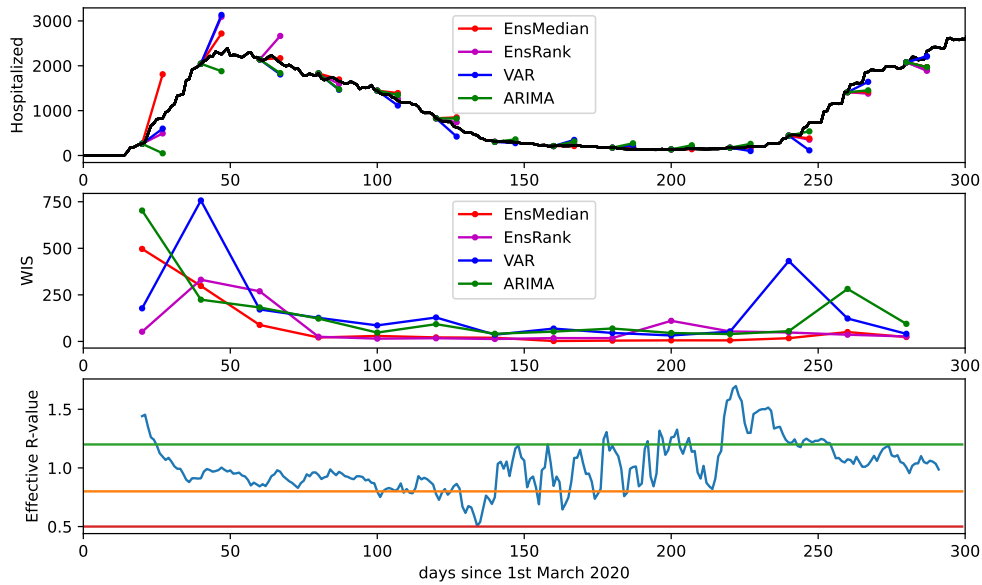


Figure 9: Evaluation of selected component model and ensemble 7-day forecasts for COVID-19 data from Sweden during 2020. A) Point predictions from the best performing ensembles (median- and adaptive rank-based) and component models (VAR and ARIMA). B) The weighted interval score (WIS) of the ensembles and models calculated from prediction intervals for each forecast. C) Estimate of effective reproduction value. The solid lines correspond to break points for the adaptive rank-based ensemble. The red line corresponds to $R_{\text{eff}} = 0.5$, the orange line to $R_{\text{eff}} = 0.8$ and the green line to $R_{\text{eff}} = 1.2$.

COVID-19 pandemic (Cramer et al., 2022). 272

In fact all models are at some point both the worst and best model. However, there are 273
individual differences where some models have distributions shifted towards higher rank 274
(e.g. Bayesian regression), whereas others are shifted towards low rank (e.g. the VAR- 275
model). The rank distributions with respect to RMSE and WIS are in general similar, 276
but Exponential regression is an exception with a distribution which is shifted towards 277
lower rank with RMSE and higher rank with WIS. The reason behind this is that WIS 278
punishes forecast with excessive confidence intervals, which the Exponential regression 279
model at times produces. 280

Taking the mean of the rank distributions (see Table 1) we notice that almost all 281
models outperform the Moving Average-model, which serves as a baseline model, the 282
exception being Linear Regression and the SIRH-Multi2, which perform worse with respect 283
to WIS at 14 day forecasts. The model performance relative to the baseline model found 284
in this study is better than the one reported in (Cramer et al., 2022), which possibly is 285
related to the larger and more diverse dataset used for evaluation. 286

Going from 7 to 14 day forecasts we note that all autoregressive models decrease 287
their relative accuracy with respect to both RMSE and WIS, whereas the mechanistic 288
models improve their accuracy. The two exponential regression models also show a slight 289
improvement for longer forecasts. The relative improvement of mechanistic models is in 290
line with previous studies that have shown that capturing transmission dynamics in the 291
model structure improves long-term accuracy (Rahmandad et al., 2022). 292

The heterogeneity of performance becomes even more evident when we stratified the 293
rank based on the effective reproduction value at the time of forecast (see fig. 4). From this 294
it can be seen that the autoregressive models in general perform better during high/very 295
high transmission compared to low/minimal. 296

This information could guide the use of different forecast models during an ongoing 297
pandemic. For example it would be possible to evaluate the performance of any set of 298
forecast models on synthetic data and stratify the accuracy based on effective reproduct- 299
ive number. The results could then inform decision-makers when considering multiple 300
forecasts. 301

As we have shown the stratification can also be used to form an adaptive rank-based 302
ensemble, where the weights of component models are adjusted depending on the instant- 303
aneous reproduction number. This rank-based ensemble outperforms all other ensemble 304
methods (see fig. 7), although the median ensemble and WIS-optimised ensemble show 305
similar performance. However, the good performance of the median ensemble, which has 306
been reported previously (Brooks et al., 2020), together with its simplicity makes it a 307
strong candidate for producing forecasts. In particular since it requires no adjustment of 308
model weights based on historical data. 309

The application of the two best ensembles on real data from Sweden during the 310
COVID-19 pandemic showed that the results from the synthetic data also hold on real 311

hospitalisation data. We see that the median and rank-based ensemble both outperform 312
the top two component models (with the lowest average rank for 7 day forecasts with WIS) 313
and that the rank-based ensemble has a lower average WIS than the median ensemble. 314

A benefit of our approach with a large-scale synthetic, yet realistic, data set is that the 315
results we obtain are more reliable compared to those obtained from a single epidemic. In 316
addition, it becomes possible to see trends in the results that are not realised in smaller 317
datasets. One notable example of this is the relation between the coefficient of variation 318
(CV) of component forecasts within an ensemble and the future error of the ensemble 319
forecast (see fig. 8). That ensemble CV is indicative of forecast error has previously been 320
observed in meteorology, where ensembles are used to account for both uncertainty in 321
initial condition and model structure (Whitaker & Lough, 1998). In meteorology, this is 322
known as the spread-skill relationship and has been shown to be informative about the 323
expected quality of the forecast. By assuming a simple statistical model for the relation- 324
ship between spread and error an upper bound on the correlation coefficient between the 325
variables can be obtained. In our data we find that for CV in the range $0 < CV < 2$ 326
the correlation coefficient between CV and MAPE-error equals 0.51, whereas the the- 327
oretical upper bound, which assumes an unbiased ensemble, equals approximately 0.6 328
(Houtekamer, 1992). However, it should be noted that the relationship between CV and 329
error is highly heteroscedastic and further analysis and validation is required before the 330
CV can be used operationally to assign confidence to ensemble forecasts. A similar re- 331
lationship was observed by Shaman & Karspeck, 2012 who made use of an ensemble 332
adjustment Kalman filter to model influenza epidemics. They used a single model for 333
disease transmission, and the ensemble was formed by multiple instances of the model 334
with different states and parameter values. In that context they showed that that the 335
logarithm of the ensemble variance was predictive of the ability of the ensemble to forecast 336
the timing of the peak of the outbreak. This is similar to our results, but yet distinct 337
since we consider a multi-model ensemble with 14 different component models. 338

This study has several limitations. To begin with we consider synthetic data generated 339
using an agent-based model of respiratory disease transmission. Although this model 340
accounts for many of the processes involved in disease transmission it might still miss 341
out on important characteristics of real data. In addition we assumed perfect access to 342
hospital data without any delays or misreporting. In realistic settings there is typically a 343
reporting delay which reduces the effective forecasting horizon. Reporting delays can be 344
handled using nowcasting methods (Bergström et al., 2022), but this introduces additional 345
uncertainty in recent data. 346

Secondly, we only consider a limited set of forecast models. Some of these models have 347
been used during the COVID-19 pandemic to predict hospital admission (Alabdulrazzaq 348
et al., 2021; Gerlee et al., 2021; Kitaoka & Takahashi, 2023; Küchenhoff et al., 2021), but 349
our study does not include other commonly used models such as age-structured compart- 350
mental models, machine learning models and agent-based models. Some of the models 351

we consider make use of additional data streams in terms of incidence and mobility, but 352
there are other data sources that can be informative when forecasting hospitalisations, 353
e.g. telenursing calls (Spreco et al., 2022) and waste-water data (Gudde et al., 2025). 354

Our study focused on hospitalised cases as the target variable, but there are a number 355
of other variables that are of interest to decision-makers during an epidemic. For example, 356
forecasting incidence can be useful since changes in incidence typically precede changes 357
in hospitalisation, thus providing an early warning signal. Also, forecasting mortality has 358
been considered useful since it provides an estimate of coming severity of an outbreak. 359

The conclusions drawn from the results concerning different ensemble methods and 360
the spread-skill relationship are based on the component models considered in this study. 361
In order to strengthen those conclusion one would like to carry out similar studies with 362
respect to both different component models and target data sets. Optimally this would be 363
performed in a prospective setting on real data. Also, our results are limited to short-term 364
forecasting and it would be interesting to see if similar results concerning ensembles are 365
obtained for longer term forecasts or even scenario projections. 366

In conclusion, this study, which is based on synthetic outbreak data, shows that fore- 367
cast model performance is heterogeneous with respect to different outbreaks and disease 368
transmission regime. We have shown that this information can be harnessed to form 369
an adaptive rank-based ensemble, which outperforms traditional ensemble types. In fu- 370
ture work we plan to investigate how well the rank-based ensemble generalises to other 371
context and how the performance depends on the amount of training data. The spread- 372
skill relationship of ensembles that we have uncovered also requires more investigation, in 373
particular in the context of other component models and datasets. 374

4. Methods 375

In this section we provide details of the data generation, the forecast models, performance 376
metrics and ensemble forecasts. All code and data are available at: [GitHub](#) 377

4.1 Data generation – CovaSim 378

To generate the synthetic outbreak data Covasim (Kerr et al., 2021), an agent-based model 379
that can simulate the transmission of a respiratory infectious disease in a population was 380
used. This model takes as an input disease- and population-specific parameters such as 381
the population size, the age distribution, the transmission probability and age-dependent 382
severity, and outputs a complete description of the outbreak, such as time-series of the 383
number of severe and asymptomatic cases, and also the effective reproduction number. 384

Covasim allows for the generation of diverse outbreaks, thanks to the large number 385
of parameters that can be given as input to the model, but also due to the possibility to 386
introduce interventions that can be planned by the user. For this work we make use of 387
non-pharmaceutical interventions in terms of a time-dependent mobility which modulates 388

the transmission probability of all contacts. We consider four different mobilities: i) 389
 actual mobility data from Sweden during the COVID-19 pandemic, ii) seasonal mobility 390
 modelled as a sine curve, iii) rapid changes to the mobility meant to represent mandatory 391
 lock-downs and iv) a constant mobility. 392

To begin with we used default settings for all parameters meaning that the disease 393
 being modelled is similar to COVID-19. The location was set to 'Sweden' which implies 394
 that the age distribution, contact networks and other population properties are set to 395
 match Swedish data. To reduce computational time we set the population size to 10^6 396
 individuals. 397

We assume that all severe and critical cases require hospital care and consider the 398
 daily number of critical and severe cases as the number of hospitalised each day. This 399
 time-series will be target for the forecast models. 400

4.2 Parameter sensitivity analysis 401

In order to generate a diverse set of outbreaks we need to define a metric that quantifies 402
 the difference between two outbreaks (in terms of time-series of hospitalised per day). 403
 Initial testing showed that it was not sufficient to simply take the absolute or squared 404
 distance between the time-series representing the hospitalisations of the two outbreaks. 405
 Given two time-series of hospitalisations Y_1 and Y_2 we opted for the following metric: 406

$$\mathcal{L}(Y_1, Y_2) = \left\| \left(\|Y_1 - Y_2\|_{L_1}, \|Y_1' - Y_2'\|_{L_1}, \|Y_1'' - Y_2''\|_{L_1}, \frac{\max(Y_1)}{\max(Y_2)}, \frac{\max(Y_1')}{\max(Y_2')}, \frac{\max(Y_1'')}{\max(Y_2'')} \right) \right\|_{L_2}, \quad (1)$$

where Y_i' and Y_i'' are the first and second numerical derivatives and $\|Y\|_{L_1} = \sum_i |Y^i|$ is 407
 the sum of absolute values of the vector Y and $\|X\|_{L_2} = \sum_i X_i^2$. It can be noted that 408
 \mathcal{L} is similar to the Sobolev norm $\|Y_1 - Y_2\|_{W^{2,1}}$ with the additional terms accounting for 409
 maximal difference in amplitude. 410

As CovaSim has a large set of inputs parameters, a first subset of key parameters was 411
 identified: the *spread* parameters and the *severity* parameters, which are parameters re- 412
 lated to disease transmission and severity. The *severity* parameters are the 4 parameters 413
 that correspond to the probability for an individual to move from one disease compart- 414
 ment to another. The *spread* parameters are 9 parameters that represent the distribution 415
 of probability of the time spend by an agent in a compartment (such as infected, crict- 416
 ical...) once it has been entered. The value of each individual is drawn from a log-normal 417
 distribution, and the *spread* parameters correspond to the mean of this log-normal dis- 418
 tribution. All the parameters have a default value of 1, which correspond to keeping the 419
 reference value. 420

This set of 13 parameters is denoted S . In order to test the forecasting models on a 421
 large, but still manageable set of different pandemics we decided to vary four parameters 422
 and that these should each take three different values in $[0.5, 1, 2]$, leading to a set of 81 423

pandemics. To select the 4 parameters in S that generated the most diversity with respect to \mathcal{L} out of the 13 possible is equivalent to solving the following problem:

$$s_{opt} = \underset{s \subset S, |s|=4}{argmax} \mathcal{H}(s),$$

with $\mathcal{H}(s) = \sum_{p_1, p_2 \in \mathcal{P}_g(s)} \mathcal{L}_2(p_1, p_2)$, and $\mathcal{P}_g(s)$ the set of the 81 pandemics generated with the 4 parameters of s . However, generating an outbreak with CovaSim is time-consuming, and it is not possible to compute the diversity of each set of 4 parameters s included in S (the set of all 13 parameters) in reasonable time.

An MCMC algorithm (Boyd et al., 2009) was therefore implemented, to perform a clever grid search on the different subsets $s \subset S$ of parameters. After 200 iterations of the MCMC algorithm, the set of parameters that maximised the diversity was found to be `[sym2sev, asym2rec, rel_symp_prob, rel_severe_prob]`.

They correspond respectively to the mean of the log-normal distribution representing the time spent in the compartment 'symptomatic' before moving into the compartment 'severe', the mean of the log-normal distribution representing the time spent in the compartment 'asymptomatic' before moving into the compartment 'recovered', to the scale factor for proportion of symptomatic cases and to the scale factor for proportion of symptomatic cases that become severe. (see (Kerr et al., 2021)).

Each of the 4 parameters was set to three different values: `[0.5, 1, 2]` and we considered the four time-dependent mobilities described above resulting in $81 \times 4 = 324$ different outbreaks.

4.3 Forecast models

In this study, we define a forecast model as a function $h_\theta(i)$, which equals the number of hospitalised cases at day i since the outbreak began, with parameters θ that are estimated by training on the data \mathcal{D} . In the training phase, $\hat{\theta}$, an estimator of θ is computed from \mathcal{D} , and used for the prediction.

We considered two types of models: univariate models which are only trained on the time series we want it to predict (the number of hospitalized in our case), and multivariate models that are trained on the time series we want to predict, but also on other time series that can be relevant to predict the number of hospitalized: the mobility and incidence (new cases/day).

Another way to classify the models is according to their underlying structure. We will consider statistical models that use time as a covariate, autoregressive models that use data from previous days as covariates and mechanistic models that are formulated as systems of coupled ordinary differential equations.

During the training or prediction phase computations sometimes fail (e.g. due to non-invertible matrices). Instead of outputting a missing value, we let the model output the value of the Moving average-model (see below), which can be interpreted as a naive

fallback when computation fails.

For a forecast that is made on day i that reaches r days into the future the model is trained on the set $\mathcal{D}_i = \{Y_j\}_{j=0}^i$. The point forecast is given by $\hat{Y}_r = h_{\hat{\theta}}(r)$ where $\hat{\theta}$ are the estimated parameter values of the model. To each point forecast we associate $(1 - \alpha)$ confidence intervals, where $\alpha = [0.02, 0.05, 0.1, 0.2, 0.3, 0.4, 0.5, 0.6, 0.7, 0.8, 0.9]$, making the forecasts probabilistic.

4.3.1 Statistical models

Exponential regression: This model assumes that the number of hospitalised cases follows $h(t, a, b, c) = ae^{b(t-c)}$, where $\theta = (a, b, c)$ are the parameters of the model and t is the number of days since the start of the outbreak. The parameters are estimated using least squares optimisation with the SciPy-function `curve_fit` and confidence intervals are computed using the Delta method (Doob, 1935).

Multivariate exponential regression: This model is similar to the univariate case and assumes that $h(t, a, b, c, d, e) = ae^{(b+dm_t+ei_t)(t-c)}$ where d and e are additional parameters, m_t is the mobility at day t and i_t is the incidence at day t . Again, we make use of least squares optimisation and the Delta method. When predictions are made we assume that the mobility and incidence take last known value for all future dates.

4.3.2 Autoregressive models

Moving average: This is the simplest of all models and serves as our baseline-model. The prediction is constant and equals the mean number of hospitalised cases in the past seven days. The confidence interval of the prediction is calculated as the standard deviation during the past seven days.

ARIMA: The $ARIMA(p, d, q)$ model is the sum of an $AR(p)$ and a $MA(q)$ model applied on the time series differentiated d times. It follows the equation:

$$Y_t^d = \alpha + \sum_{i=1}^p \beta_{t-i} Y_{t-i}^d + \sum_{j=1}^q \phi_{t-j} \epsilon_{t-j},$$

where Y_t^d is the time series at time t , d is the order of the differentiation, α is a constant, p is the order of the autoregressive part, q is the order of the moving average part and ϵ_{t-j} is the difference between the prediction of the model and the real value at time $t - j$.

The coefficients are estimated through maximum likelihood estimation. This method is implemented in the `statsmodels` library, which directly provides prediction and confidence intervals. We performed a grid search on a single pandemic to identify the combination of parameters that would optimize the prediction accuracy. We found an optimal value for $p = 3, d = 0, q = 3$.

VAR: The VAR model is a multivariate AR-model, where several variables are predicted. This model exploits the correlation between variables. Let $Y_{1,t}, \dots, Y_{k,t}$ be the

times series (in our case, $k = 3$ and they correspond to the number of hospitalized, the number of infected and the mobility at day t).

$$\text{VAR}(p) : \begin{pmatrix} Y_{1,t} \\ Y_{2,t} \\ \vdots \\ Y_{k,t} \end{pmatrix} = \begin{pmatrix} c_1 \\ c_2 \\ \vdots \\ c_k \end{pmatrix} + \begin{pmatrix} \phi_{11,1} & \phi_{12,1} & \cdots & \phi_{1k,1} \\ \phi_{21,1} & \phi_{22,1} & \cdots & \phi_{2k,1} \\ \vdots & \vdots & \ddots & \vdots \\ \phi_{k1,1} & \phi_{k2,1} & \cdots & \phi_{kk,1} \end{pmatrix} \begin{pmatrix} Y_{1,t-1} \\ Y_{2,t-1} \\ \vdots \\ Y_{k,t-1} \end{pmatrix} \\ + \cdots + \begin{pmatrix} \phi_{11,p} & \phi_{12,p} & \cdots & \phi_{1k,p} \\ \phi_{21,p} & \phi_{22,p} & \cdots & \phi_{2k,p} \\ \vdots & \vdots & \ddots & \vdots \\ \phi_{k1,p} & \phi_{k2,p} & \cdots & \phi_{kk,p} \end{pmatrix} \begin{pmatrix} Y_{1,t-p} \\ Y_{2,t-p} \\ \vdots \\ Y_{k,t-p} \end{pmatrix} + \begin{pmatrix} \epsilon_{1,t} \\ \epsilon_{2,t} \\ \vdots \\ \epsilon_{k,t} \end{pmatrix}$$

Again, the $\phi_{i,j,k}$ and c_i are estimated through maximum likelihood estimation with the `statsmodel` library. The confidence intervals are also directly provided by the library.

Linear regression: This is an AR-model where the parameters are estimated using linear regression. In order to implement this model we converted the time-series $Y_{t,t \in \{1, \dots, n\}}$ into a training set (X_i, Y_i) such that: $\forall i \in \{1, \dots, n\}, X_i = (Y_{i-1}, Y_{i-2}, \dots, Y_{i-20})$, which implies that the order of the model equals $p = 20$. The model was implemented using the `scikit-learn` package.

The confidence interval for the linear regression prediction was computed as follows: Let us suppose that the data follows a linear regression model: $Y = X\beta + \epsilon$, with $Y \in \mathbb{R}^n$, $X \in \mathbb{R}^{n \times d}$, $\beta \in \mathbb{R}^d$ and $\epsilon \sim \mathcal{N}(0, \sigma^2)$. The least square estimator of β is $\hat{\beta} = (X^T X)^{-1} X^T Y$. If we create a new matrix \tilde{X} with unseen data, we can perform the prediction as follow:

$$\begin{aligned} \tilde{Y} &= \tilde{X} \hat{\beta} \\ &= \tilde{X} (X^T X)^{-1} X^T Y \\ &= \tilde{X} (X^T X)^{-1} X^T (X\beta + \epsilon) \\ &= \tilde{X} \beta + \tilde{X} (X^T X)^{-1} X^T \epsilon. \end{aligned}$$

This implies that \tilde{Y} follows a normal distribution of expected value $\tilde{X} \beta$ and variance $\tilde{X} (X^T X)^{-1} \tilde{X}^T \sigma^2$.

Bayesian regression: This model is similar to linear regression, and also implemented using the `scikit-learn` package, but the parameters are estimated using Bayesian ridge regression.

The Bayesian ridge regression model treats the problem of predicting the future number of severe cases as a linear regression problem, where past observations serve as covariates. The default setting is to use data stretching 20 days into the past to predict the number of severe cases tomorrow, i.e.

$$\hat{Y}_{t+1} = w_0 + w_1 Y_t + \dots + w_p Y_{t-19} + \epsilon_t$$

where \hat{Y}_{t+1} is the predicted number of severe cases at day t , Y_{t-i} is the number of severe cases i days prior, w_i are the weights, which are estimated using historical data, and ε_t is Gaussian noise with mean zero and variance λ^{-1} .

The weights follow a Gaussian prior:

$$P(w|\alpha) \sim \mathcal{N}(0, \alpha^{-1}I),$$

where α is the prior precision, controlling the regularization strength.

The likelihood of the observed data given the weights is Gaussian:

$$P(y|X, w, \lambda) \sim \mathcal{N}(X \cdot w, \lambda^{-1}I),$$

. Both the weights and the values of α and λ are estimated using Bayesian inference.

4.3.3 Mechanistic models

SIRH: The SIRH-model is an extension of the classic compartmental SIR (Susceptible-Infectious-Recovered) model used to describe the spread of infectious diseases. In the SIRH model, a fourth compartment, H for Hospitalised, is added. The evolution of the number of individuals in each compartment is described by a system of coupled ordinary differential equations:

$$\begin{cases} \frac{dS}{dt} = -\beta \frac{SI}{N} \\ \frac{dI}{dt} = \beta \frac{SI}{N} - \gamma_i I - hI \\ \frac{dR}{dt} = \gamma_i I + \gamma_h h \\ \frac{dH}{dt} = hI - \gamma_h H \end{cases} \quad (2)$$

At $t = 0$, the values of (S_0, I_0, R_0, H_0) are fixed to $(10^6 - 1, 1, 0, 0,)$, corresponding to a single infectious individual in a otherwise susceptible population. The equations were solved using the SciPy-function `odeint`.

To train this model, we minimize the least squares error between the number of hospitalised cases in the training data and $H(t)$ with respect to $\theta = (\beta, \gamma_i, \gamma_h, h)$, using `curve_fit`. We implemented four version of the SIRH-model in which either γ_i, γ_h were fixed or subject to optimisation. (see the Table.2). If fixed they were set to $\gamma_i = 1/8$ and $\gamma_h = 1/18$, which is in line with the mean number of days for recovery for regular and severe cases in CovaSim.

For a prediction made at day t with reach r we solve the model numerically with the above mentioned initial condition with the parameters $\hat{\theta}$ computed during the training phase. The prediction is shifted so that it equals the observed number of hospitalised cases at day t , i.e. $H(t) = Y_t$. The confidence interval of the prediction is computed using the Delta method and numerical differentiation.

	γ_i	γ_h
SIRH1	1/8	1/18
SIRH2	1/8	free
SIRH3	free	1/18
SIRH4	free	free

Table 2: Difference between the SIRH models

SIRH-Multi: We also implemented two SIRH-models where the mobility data influences the contact rate. We assume that β varies with the time as a linear combination of the mobility: $\beta_t = a + b \times m_t$, similar to what was used in (Gerlee et al., 2021).

We consider two versions of the SIRH-Multi model in which the values of γ_h and γ_i are either fixed or subject to optimisation. SIRH-Multi1 refers to the model in which γ_h and γ_i are free and SIRH-Multi2 refers to the model in which they are fixed to $\gamma_i = 1/8$ and $\gamma_h = 1/18$.

SEIR-Mob: This model is adapted directly from (Gerlee et al., 2021) and consists of an SEIR-model with time-dependent mobility of the form $\beta_t = a + b \times m_t$. The model assumes that a fraction p of the infected cases become hospitalised with a delay of 21 days. To train the model, we minimize the least squares error between the number of hospitalised cases in the training data and the model solution with respect to $\theta = (a, b, p)$, using `curve_fit`. Model prediction and confidence intervals are computed as for the SIRH-models.

4.4 Performance metrics

Two metrics were used to assess the performance of the models. The first metric is the Weighted Interval Score (WIS), which is a metric commonly used in forecast evaluation (Cramer et al., 2022).

Let α be in $]0, 1[$. Let \hat{y} be the prediction of the model and y the real value. Let $[l, u]$ be the $(1 - \alpha)$ confidence interval of the prediction. The Interval Score (IS) is defined as

$$IS_\alpha([l, u], y) = \frac{2}{\alpha} \times (\mathbb{1}_{\{y < l\}}(l - y) + \mathbb{1}_{\{y > u\}}(y - u) + (u - l)).$$

This metric consists of three terms: a term of overprediction that punishes a model with a confidence interval at level α which is above the real value, a term of underprediction that punishes a model whose confidence interval is under the real value, and a term of range, that punishes too wide confidence intervals.

Let $(\alpha_k)_{k \in \{1, \dots, K\}} \in]0, 1[^K$ be a sequence of significance levels. The WIS is now defined as

$$WIS([l, u], \hat{y}, y) = w_0 |y - \hat{y}| + \sum_{k=1}^K w_k IS_{\alpha_k}([l, u], y),$$

with weights $(w_k)_{k \in \{1, \dots, K\}} \in \mathbb{R}_+^K$ chosen by the user.

According to previous literature (Cramer et al., 2022), we decided to set 574
 $(\alpha_k)_{k \in \{1, \dots, K\}} = [1, 0.02, 0.05, 0.1, 0.2, 0.3, 0.4, 0.5, 0.6, 0.7, 0.8, 0.9]$ and $\forall k \in \{1, \dots, K\}, w_k =$ 575
 $\frac{\alpha_k}{2}$. 576

The second metric is the Root Mean Square Error (RMSE). With the same notations 577
as above, we define the RMSE as 578

$$\text{RMSE}(\hat{y}, y) = \sqrt{(y - \hat{y})^2}$$

This metric focuses on the point prediction, and does not take into account the confidence 579
intervals. 580

The models were tested on all the 324 pandemics, on 14 data points different (at 581
days 20, 40, 60, ..., 280). For each individual point, the models were trained on the 582
previous days of the pandemic. A 7 and 14 days ahead point prediction was computed, 583
and $[0.02, 0.05, 0.1, 0.2, 0.3, 0.4, 0.5, 0.6, 0.7, 0.8, 0.9]$ confidence-intervals were constructed. 584
The WIS and the RMSE of these predictions were then calculated. For the analysis of 585
the results, we decided to remove the points for which the number of hospitalized was 586
below 10, (i.e less than 10^{-4} hospitalized per 100 000 citizens). The reason being that 587
it is of little use to assess the performances of the models during the period in which 588
hospitalisations and incidence are low. Not removing those points would lead to biased 589
results, as points of low hospitalisations represent 44% of the dataset, and we would have 590
concluded that the best model is the one that performs well when there is no or very little 591
transmission. 592

4.5 Classifying stages of the epidemic 593

In order to compare the performance of the models at different stages of an outbreak, we 594
classified each day of the outbreak into five categories based on the effective reproduction 595
number R_{eff} . This number was extracted from the CovaSim simulations. The classification 596
was made according Table 3. 597

Condition	Classification
$R_{\text{eff}} < 0.5$	minimal transmission
$0.5 \leq R_{\text{eff}} < 0.8$	low transmission
$0.8 \leq R_{\text{eff}} < 1.2$	stable
$1.2 \leq R_{\text{eff}} < 3$	high transmission
$R_{\text{eff}} \geq 3$	very high transmission

Table 3: Classification according to reproduction number.

Among all 2549 points where model predictions were evaluated, 698 were classified as 598
‘minimal transmission’, 579 as ‘low transmission’, 388 as ‘stable’, 752 as ‘high transmis- 599
sion’, 132 as ‘very high transmission’. 600

4.6 The ensemble model

601

This section describes how the ensemble forecast were computed. The dataset of hospitalisation curves was randomly split into a training set and evaluation set where each was assigned to the training set with probability 0.5. Training of the ensemble weights was only performed on the training set.

602

603

604

605

Average Ensemble (EnsAvg): this ensemble takes an unweighted mean of all component models to calculate the point prediction. The positions of the upper and lower confidence intervals for each significance level were also computed as an unweighted mean.

606

607

608

Median Ensemble (EnsMedian): this ensemble uses the median of all point predictions. The positions of the upper and lower confidence intervals for each significance level were also computed using the median.

609

610

611

Regression Ensemble (EnsReg): this ensemble takes a weighted mean of the component point predictions plus an intercept

612

613

$$Y_t^E = w_0 + \sum_{k=1}^{14} w_k \hat{Y}_t^k \quad (3)$$

The weights w_k and intercept w_0 were obtained using linear regression where the actual hospitalisation on day t is the target variable. The positions of the upper and lower confidence intervals for each significance level were also computed according to (3).

614

615

616

RMSE-optimised Ensemble (EnsRMSE): This ensemble is similar to EnsReg, but considers weights that sum to unity and no intercept. The weights are obtained by minimising the function

617

618

619

$$E_{\text{RMSE}}(\mathbf{w}) = \sum_{i=1}^{N_T} \sum_{j=1}^{15} \text{RMSE}(Y_{i,j}, \sum_{k=1}^{14} w_k \hat{Y}_{i,j}^k) \quad (4)$$

subject to the constraint $\sum_k w_k = 1$. Here the double sum runs over all outbreaks in the training set and across all forecasts within a given outbreak, $\hat{Y}_{i,j}$ is the observed number of hospitalised cases and $\hat{Y}_{i,j}^k$ is the forecast of model k . The optimisation problem is solved using the SciPy-function `minimize` with the trustconst-method and an initial guess equal to 1/14 for all w_k .

620

621

622

623

624

WIS-optimised Ensemble (EnsWIS): This ensemble is similar to EnsRMSE with the difference that it is the WIS which is optimised. Therefore we minimise the function

625

626

$$E_{\text{WIS}}(\mathbf{w}) = \sum_{i=1}^{N_T} \sum_{j=1}^{15} \text{WIS}([\sum_{k=1}^{14} w_k l_{i,j}^k, \sum_{k=1}^{14} w_k u_{i,j}^k], \hat{Y}_{i,j}, \sum_{k=1}^{14} w_k Y_{i,j}^k) \quad (5)$$

subject to the constraint $\sum_k w_k = 1$. The optimisation problem is solved using the SciPy-function `minimize` with the trustconst-method and an initial guess equal to 1/14 for all w_k .

627

628

629

Rank-based Ensemble (EnsRank): this ensemble changes its weights depending on the current effective reproductive number. For each of the five regimes defined in fig. 3 we pick the five models with the smallest average rank $r_1 < r_2 < \dots < r_5$. We now set $\tilde{w}_k = 1/r_k$ and normalise the weights so that the sum to unity according to

$$w_k = \tilde{w}_k / \sum_{i=1}^5 \tilde{w}_i.$$

The forecast of this ensemble equals

$$Y_t^R = \sum_{k=1}^5 w_k Y_t^k$$

where the sum runs over the top-ranked models given the current effective reproduction number.

4.7 Ensemble variance

To investigate the relationship between the variation of component model forecasts and ensemble error we calculated the coefficient of variation for all ensemble forecast across all outbreaks. The coefficient of variation is defined according to $CV = \sigma/\mu$ where $\mu = \frac{1}{14} \sum_{k=1}^{14} \hat{Y}^k$ is the mean prediction and $\sigma = \frac{1}{14} \sum_{k=1}^{14} (\mu - \hat{Y}^k)^2$. The ensemble error was calculated for the median ensemble using the Mean Absolute Percentage Error $MAPE_t = |Y_t - Y_t^M|/Y_t$, where Y_t is the outcome and Y_t^M is the median forecast at time t . For the analysis we exclude points where $Y_t < 10$.

4.8 Evaluation on Swedish data

In order to obtain good estimates of the effective reproduction number for COVID-19 during the pandemic in Sweden in 2020 we estimated incidence based on COVID-19 deaths according to the method presented in (Wacker et al., 2021). Data on deaths were obtained from the Swedish National Board of Welfare. The effective reproduction number was estimated using the method described in (Cori et al., 2013), with which estimation of R_{eff} on a given day only uses historical data. The generation time distribution required for the estimation was obtained from (Knight & Mishra, 2020).

Author Contributions

Grégoire Béchade: Methodology, Software, Formal analysis, Investigation, Writing - Original Draft, Writing - Review & Editing. Tobjörn Lundh: Methodology, Writing - Review & Editing. Philip Gerlee: Conceptualization, Methodology, Software, Formal analysis, Investigation, Writing - Review & Editing, Visualization, Supervision.

Data Availability 658

All code and data used in this study is available at [GitHub](#). 659

Acknowledgments 660

The authors would like to thank Matthew Biggerstaff at the Centers for Disease Control and Prevention for suggesting the link between ensemble variance and accuracy. 661
662

References 663

- Alabdulrazzaq, H., Alenezi, M. N., Rawajfih, Y., Alghannam, B. A., Al-Hassan, A. A., & Al-Anzi, F. S. (2021). On the accuracy of arima based prediction of covid-19 spread. *Results in Physics*, 27, 104509. 664
665
666
- Bergström, F., Günther, F., Höhle, M., & Britton, T. (2022). Bayesian nowcasting with leading indicators applied to covid-19 fatalities in sweden. *PLOS Computational Biology*, 18(12), e1010767. 667
668
669
- Boyd, S., Diaconis, P., Parrilo, P., & Xiao, L. (2009). Fastest mixing markov chain on graphs with symmetries. *SIAM Journal on Optimization*, 20(2), 792–819. 670
671
- Bracher, J., Ray, E. L., Gneiting, T., & Reich, N. G. (2021). Evaluating epidemic forecasts in an interval format. *PLoS computational biology*, 17(2), e1008618. 672
673
- Brooks, L. C., Ray, E. L., Bien, J., Bracher, J., Rumack, A., Tibshirani, R. J., & Reich, N. G. (2020). Comparing ensemble approaches for short-term probabilistic covid-19 forecasts in the us. *International Institute of Forecasters*, 39. 674
675
676
- Cori, A., Ferguson, N. M., Fraser, C., & Cauchemez, S. (2013). A new framework and software to estimate time-varying reproduction numbers during epidemics. *American journal of epidemiology*, 178(9), 1505–1512. 677
678
679
- Cramer, E. Y., Huang, Y., Wang, Y., Ray, E. L., Cornell, M., Bracher, J., Brennen, A., Castro Rivadeneira, A. J., Gerding, A., House, K., Jayawardena, D., Kanji, A. H., Khandelwal, A., Le, K., Niemi, J., Stark, A., Shah, A., Wattanachit, N., Zorn, M. W., ... Consortium, U. C.-1. F. H. (2021). The united states covid-19 forecast hub dataset. *medRxiv*. <https://doi.org/10.1101/2021.11.04.21265886> 680
681
682
683
684
- Cramer, E. Y., Ray, E. L., Lopez, V. K., Bracher, J., Brennen, A., Castro Rivadeneira, A. J., Gerding, A., Gneiting, T., House, K. H., Huang, Y., et al. (2022). Evaluation of individual and ensemble probabilistic forecasts of covid-19 mortality in the united states. *Proceedings of the National Academy of Sciences*, 119(15), e2113561119. 685
686
687
688
689
- Doob, J. L. (1935). The limiting distributions of certain statistics. *The Annals of Mathematical Statistics*, 6(3), 160–169. 690
691

- Fox, S. J., Lachmann, M., Tec, M., Pasco, R., Woody, S., Du, Z., Wang, X., Ingle, T. A., Javan, E., Dahan, M., et al. (2022). Real-time pandemic surveillance using hospital admissions and mobility data. *Proceedings of the National Academy of Sciences*, 119(7), e2111870119.
- Gerlee, P., Karlsson, J., Fritzell, I., Brezicka, T., Spreco, A., Timpka, T., Jöud, A., & Lundh, T. (2021). Predicting regional covid-19 hospital admissions in sweden using mobility data. *Scientific Reports*, 11(1), 24171.
- Gudde, A., Krosgaard, L. W., Benedetti, G., Schierbech, S. K., Brokhattingen, N., Petrovic, K., Rasmussen, L. D., Franck, K. T., Ethelberg, S., Larsen, N. B., et al. (2025). Predicting hospital admissions due to covid-19 in denmark using wastewater-based surveillance. *Science of The Total Environment*, 966, 178674.
- Houtekamer, P. (1992). The quality of skill forecasts for a low-order spectral model. *Monthly weather review*, 120(12), 2993–3002.
- Kerr, C. C., Stuart, R. M., Mistry, D., Abeysuriya, R. G., Rosenfeld, K., Hart, G. R., Núñez, R. C., Cohen, J. A., Selvaraj, P., Hagedorn, B., et al. (2021). Covasim: An agent-based model of covid-19 dynamics and interventions. *PLOS Computational Biology*, 17(7), e1009149.
- Kitaoka, T., & Takahashi, H. (2023). Improved prediction of new covid-19 cases using a simple vector autoregressive model: Evidence from seven new york state counties. *Biology Methods and Protocols*, 8(1), bpac035.
- Knight, J., & Mishra, S. (2020). Estimating effective reproduction number using generation time versus serial interval, with application to covid-19 in the greater toronto area, canada. *Infectious Disease Modelling*, 5, 889–896.
- Kobres, P.-Y., Chretien, J.-P., Johansson, M. A., Morgan, J. J., Whung, P.-Y., Mukundan, H., Del Valle, S. Y., Forshey, B. M., Quandelacy, T. M., Biggerstaff, M., et al. (2019). A systematic review and evaluation of zika virus forecasting and prediction research during a public health emergency of international concern. *PLoS neglected tropical diseases*, 13(10), e0007451.
- Küchenhoff, H., Günther, F., Höhle, M., & Bender, A. (2021). Analysis of the early covid-19 epidemic curve in germany by regression models with change points. *Epidemiology & Infection*, 149, e68.
- Lutz, C. S., Huynh, M. P., Schroeder, M., Anyatonwu, S., Dahlgren, F. S., Danyluk, G., Fernandez, D., Greene, S. K., Kipshidze, N., Liu, L., et al. (2019). Applying infectious disease forecasting to public health: A path forward using influenza forecasting examples. *BMC Public Health*, 19, 1–12.
- Munday, J. D., Rosello, A., Edmunds, W. J., & Funk, S. (2024). Forecasting the spatial spread of an ebola epidemic in real-time: Comparing predictions of mathematical models and experts. *eLife*, 13.

- Nixon, K., Jindal, S., Parker, F., Reich, N. G., Ghobadi, K., Lee, E. C., Truelove, S., & Gardner, L. (2022). An evaluation of prospective covid-19 modelling studies in the usa: From data to science translation. *The Lancet Digital Health*, 4(10), e738–e747.
- Rahmandad, H., Xu, R., & Ghaffarzadegan, N. (2022). Enhancing long-term forecasting: Learning from covid-19 models. *PLoS computational biology*, 18(5), e1010100.
- Ray, E. L., Brooks, L., Bien, J., Bracher, J., Gerding, A., Rumack, A., Biggerstaff, M., Johansson, M., Tibshirani, R., & Reich, N. (2021). Challenges in training ensembles to forecast covid-19 cases and deaths in the united states. *International Institute of Forecasters*.
- Ray, E. L., Brooks, L. C., Bien, J., Biggerstaff, M., Bosse, N. I., Bracher, J., Cramer, E. Y., Funk, S., Gerding, A., Johansson, M. A., et al. (2023). Comparing trained and untrained probabilistic ensemble forecasts of covid-19 cases and deaths in the united states. *International journal of forecasting*, 39(3), 1366–1383.
- Reich, N. G., Brooks, L. C., Fox, S. J., Kandula, S., McGowan, C. J., Moore, E., Osthus, D., Ray, E. L., Tushar, A., Yamana, T. K., et al. (2019). A collaborative multi-year, multimodel assessment of seasonal influenza forecasting in the united states. *Proceedings of the National Academy of Sciences*, 116(8), 3146–3154.
- Reich, N. G., Lessler, J., Funk, S., Viboud, C., Vespignani, A., Tibshirani, R. J., Shea, K., Schienle, M., Runge, M. C., Rosenfeld, R., et al. (2022). Collaborative hubs: Making the most of predictive epidemic modeling.
- Shaman, J., & Karspeck, A. (2012). Forecasting seasonal outbreaks of influenza. *Proceedings of the National Academy of Sciences*, 109(50), 20425–20430.
- Spreco, A., Jöud, A., Eriksson, O., Soltesz, K., Källström, R., Dahlström, Ö., Eriksson, H., Ekberg, J., Jonson, C.-O., Fraenkel, C.-J., et al. (2022). Nowcasting (short-term forecasting) of covid-19 hospitalizations using syndromic healthcare data, sweden, 2020. *Emerging Infectious Diseases*, 28(3), 564.
- Taylor, J. W., & Taylor, K. S. (2023). Combining probabilistic forecasts of covid-19 mortality in the united states. *European Journal of Operational Research*, 304(1), 25–41.
- Wacker, A., Jöud, A., Bernhardsson, B., Gerlee, P., Gustafsson, F., & Soltesz, K. (2021). Estimating the sars-cov-2 infected population fraction and the infection-to-fatality ratio: A data-driven case study based on swedish time series data. *Scientific Reports*, 11(1), 23963.
- Whitaker, J. S., & Loughie, A. F. (1998). The relationship between ensemble spread and ensemble mean skill. *Monthly weather review*, 126(12), 3292–3302.

Supplementary Information for “Evaluation of
respiratory disease hospitalisation forecasts using
synthetic outbreak data”

Grégoire Béchade^{1,*}, Torbjörn Lundh², and Philip Gerlee³

¹Ecolé Polytechnique, gregoire.bechade@polytechnique.edu

²Department of Mathematical Sciences, Chalmers University of Technology & University of
Gothenburg, Sweden, torbjorn.lundh@chalmers.se

³Department of Mathematical Sciences, Chalmers University of Technology & University of
Gothenburg, Sweden gerlee@chalmers.se

*Corresponding author: Grégoire Béchade

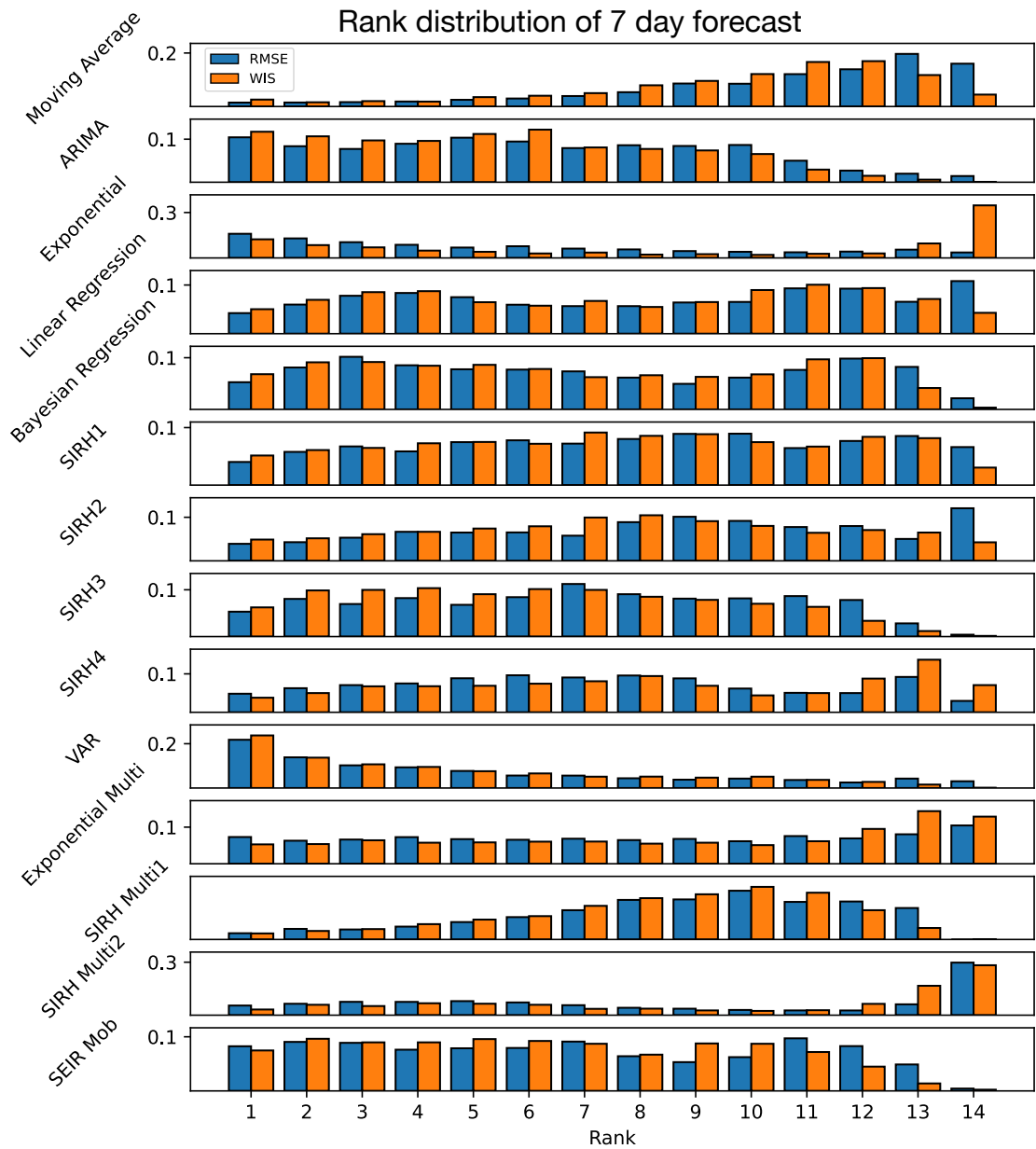


Figure 1: Distribution of rankings of the models for all points for 7-day forecasts with respect to both RMSE and WIS.

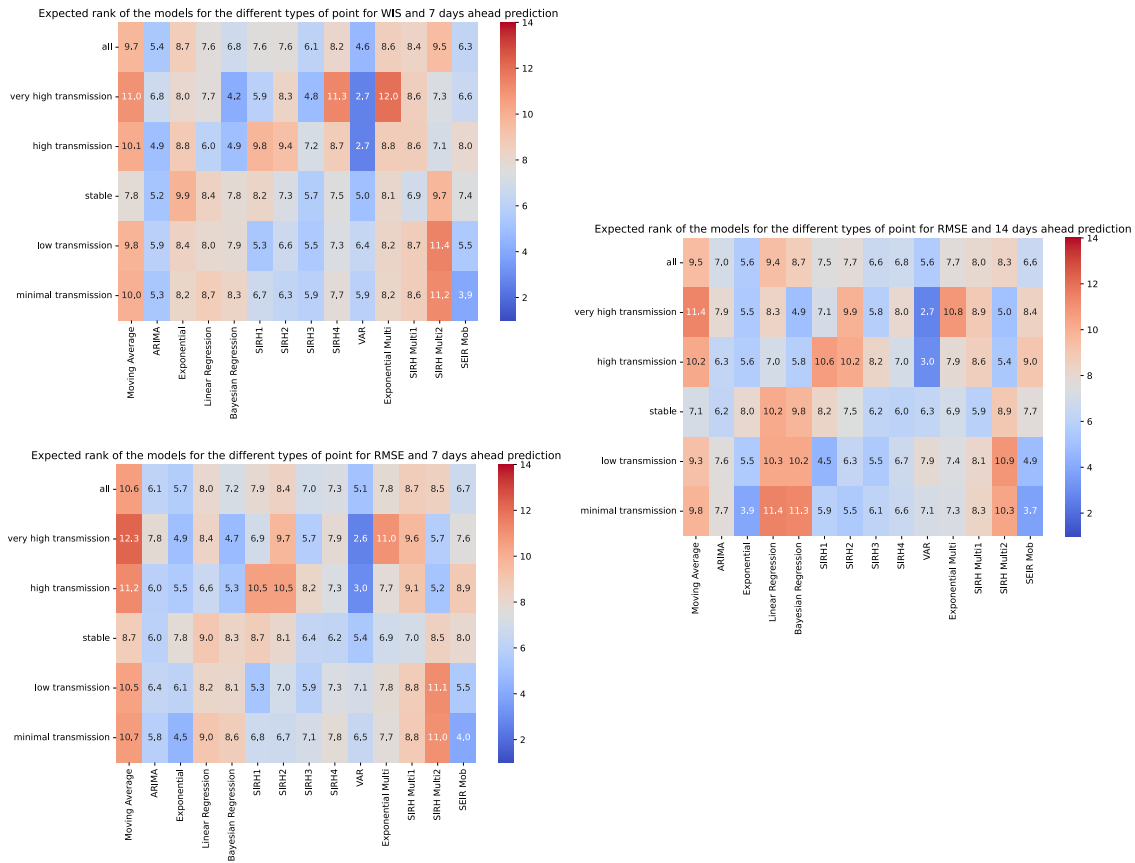


Figure 2: Heatmap of model performance based on RMSE and WIS for 7- and 14-day forecasts. The day of forecast is classified according to the current effective reproduction number according to: minimal transmission ($R_{\text{eff}} < 0.5$), low transmission ($0.5 \leq R_{\text{eff}} < 0.8$), stable ($0.8 \leq R_{\text{eff}} < 1.2$), high transmission ($1.2 \leq R_{\text{eff}} < 3$) and very high transmission $R_{\text{eff}} \geq 3$.

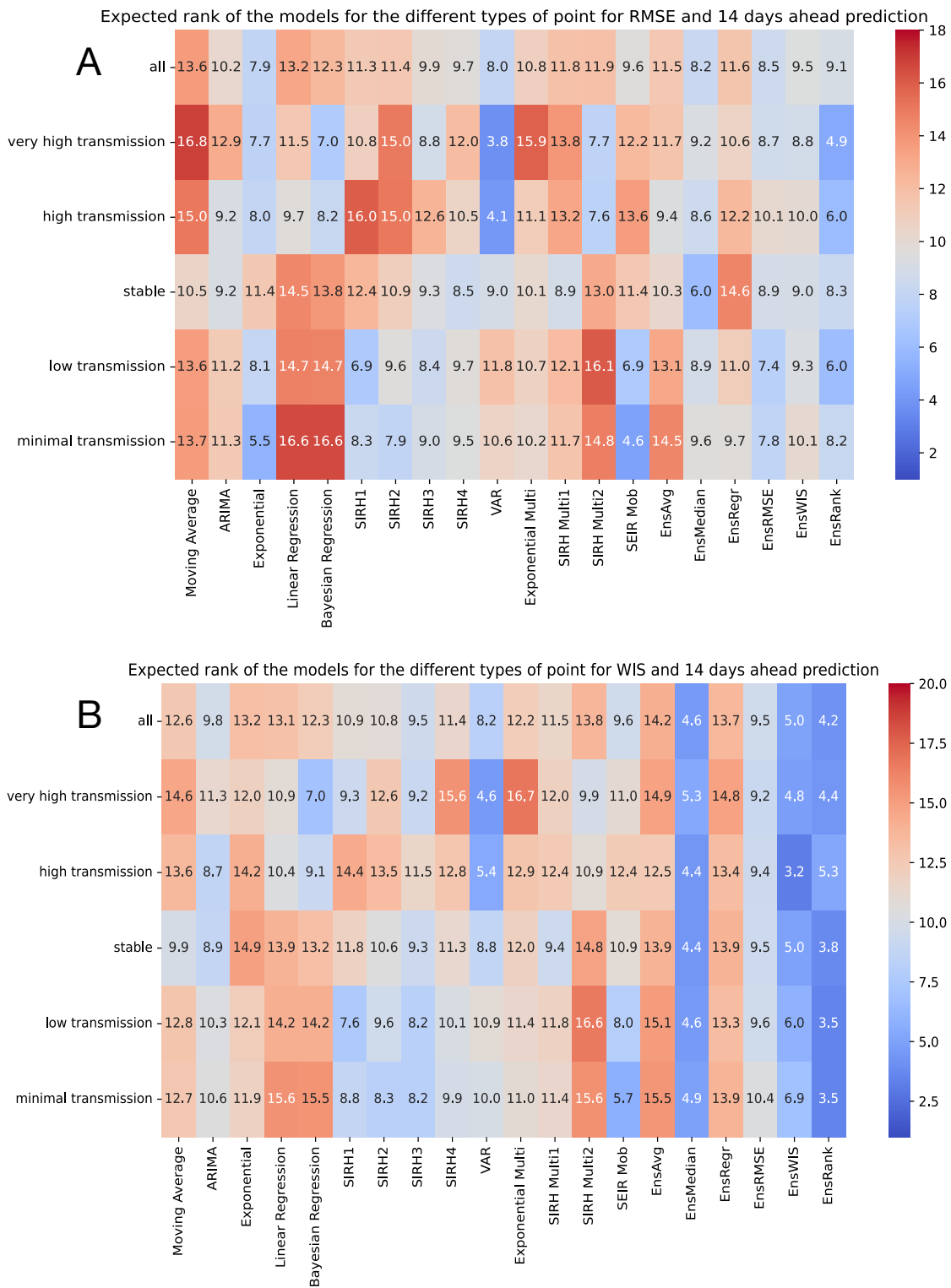


Figure 3: The average ensemble rank as compared to both component models and the six ensembles for A) RMSE and B) WIS.

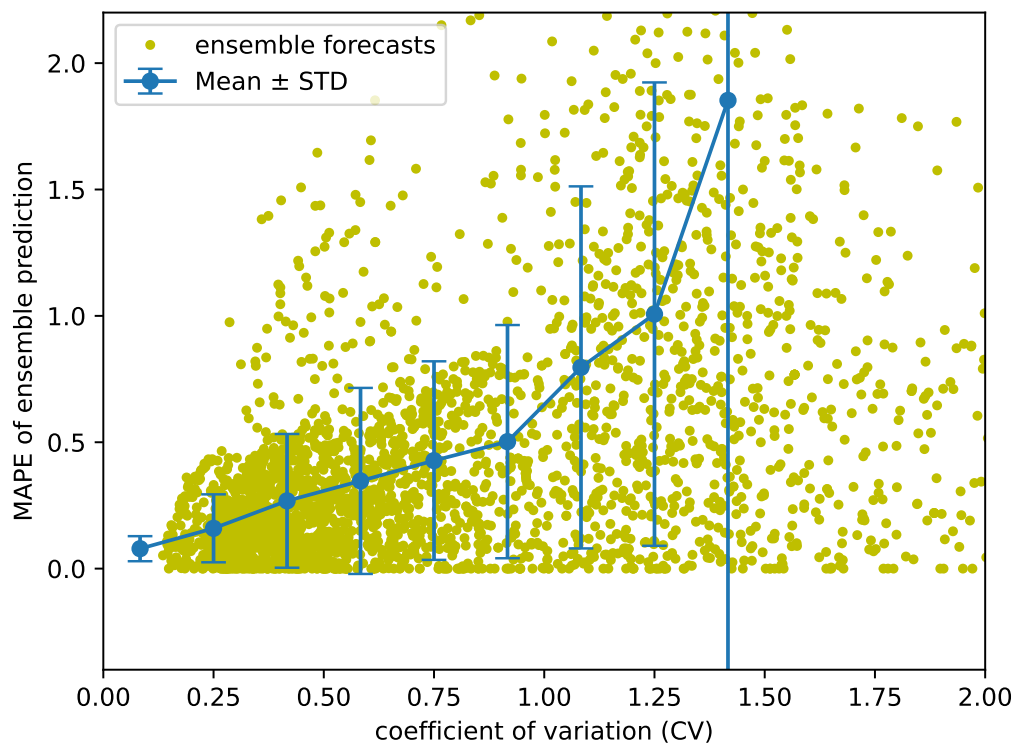


Figure 4: The coefficient of variation (CV) of the individual model predictions for 14-day forecasts and the corresponding error (MAPE) of the Median Ensemble prediction. The solid line shows the mean MAPE in each bin and the error bars correspond to one standard deviation.